

Propagation in erbium and silicon codoped silica slab waveguides: analysis of gain

This article has been downloaded from IOPscience. Please scroll down to see the full text article.

2004 J. Phys.: Condens. Matter 16 6627

(<http://iopscience.iop.org/0953-8984/16/36/028>)

View [the table of contents for this issue](#), or go to the [journal homepage](#) for more

Download details:

IP Address: 129.252.86.83

The article was downloaded on 27/05/2010 at 17:27

Please note that [terms and conditions apply](#).

Propagation in erbium and silicon codoped silica slab waveguides: analysis of gain

C Dufour¹, M Levalois¹, M Prassas², B Garrido³, J Moreno³ and R Rizk¹

¹ SIFCOM–ENSICAEN (ex LERMAT), UMR CNRS 6176, 6 Boulevard du Maréchal Juin, 14050 CAEN Cedex, France

² Corning SA Fontainebleau Research Center, Inorganic Materials Group, 7 bis avenue de Valvins, 77210 Avon, France

³ Universitat de Barcelona, Departament d'Electrònica, Carrer Martí i Franquès, 1 08028 Barcelona, Spain

E-mail: christian.dufour@ismra.fr

Received 5 April 2004

Published 27 August 2004

Online at stacks.iop.org/JPhysCM/16/6627

doi:10.1088/0953-8984/16/36/028

Abstract

The feasibility of optical amplifying waveguides is investigated through the elaboration of silica films codoped with erbium ions and silicon nanograins. The waveguiding function is provided by the index contrast between the active and cladding layers whereas the amplification is achieved by an efficient interaction between silicon nanograins and erbium ions. Based on experimental results and theoretical studies, this paper aims at providing a detailed analysis of the optical gain expected in slab waveguides taking into account a lateral pumping scheme of the silicon nanograins, the energy transfer mechanism from silicon grains to erbium ions and finally the propagation equations within the active layer. The main parameters—such as erbium and silicon concentrations, device length and pumping power—have been examined.

Introduction

In the field of photonics, a huge amount of work has been devoted to the development of optically active materials that could be used as waveguide amplifiers. The most promising devices are based on erbium-doped silica thin films containing silicon nanograins. A comprehensive review of this research field has been given by Kik and Polman [1]. Silica is well adapted to the optical communication of a commonly used 1.54 μm signal since the linear losses are minimal at this wavelength. The optical properties of silicon rich silica films have been well investigated [2–7], giving the knowledge necessary to understand the luminescence features of such films doped with erbium. The purpose is to integrate an optical amplifier structure in a waveguide in order for it to be compact and usable for metropolitan or even home optical communications. The scientific community must now face two challenges:

(i) one has to deal with the amplifying properties based on an efficient energy transfer between silicon nanograins and erbium ions [8–13]; (ii) once the active layer is elaborated, the optical index as well as the geometrical dimensions must lead to a good confinement of the signal [14] so that the output to input energy ratio is maximum. The first point has been investigated since the work published by Fujii *et al* [9]. A thorough knowledge is being acquired of the influence of the parameters (erbium and silicon concentrations, silicon grain size) on the photoluminescence properties (intensity and lifetimes of erbium excited levels). The second point is the goal of the EU contract (SINERGIA) referenced in the acknowledgments section. SINERGIA intends to realize a small-size, high-performance and low-cost waveguide amplifier from silica or other specific glass co-doped with Er and Si nanocrystals. A recent work has proposed a review on erbium implanted silicon–silica film luminescence properties [15]. A comprehensive set of parameters extracted from experimental data is used to solve the population equations of the different erbium levels N_1 and N_2 which are respectively the ground level and the first excited level. $N_{\text{er}} = N_1 + N_2$ is the total erbium concentration. The local gain is simulated as a function of the pumping power and the inversion coefficient $(N_2 - N_1)/N_0$.

The main objective of the present paper is to give an overall understanding of the gain properties of slab waveguides taking into account a complete set of equations including not only the excitons and erbium level population equations but also the propagation equations of a 1.54 μm signal along the guide leading to the simulation of a real gain—i.e. the output to input signal ratio—and the noise figure derived from amplified spontaneous emission. The theoretical work developed hereafter represents one of the four technical workpackages in the SINERGIA framework.

1. Theoretical background

The amplification of a 1.54 μm optical signal is considered through the scheme described in figure 1. An active layer—constituted of silica containing erbium ions and silicon nanograins—is sandwiched between cladding layers whose optical index is lower than that of the active layer so that the optical signal can be guided along the structure. The layers thicknesses given in figure 1 have been taken from the very first samples that have been tested and for which a positive gain has been measured. The upper cladding layer is etched so that a rib appears on the top of the device. The rib characteristics (height and width) allow the control of both the field confinement and the number of modes that can be transmitted. The feasibility of such a device is still being demonstrated either by authors like Han *et al* [16] or by co-workers in the framework of the SINERGIA contract quoted in the introduction section. The amplification is based on a silicon-to-erbium energy transfer mechanism [17] which we briefly describe in the following lines. The signal is amplified in the regions where the erbium excited level population inversion occurs. This inversion is achieved by using a pumping light source ($\lambda = 488 \text{ nm}$) whose intensity is mainly absorbed by the silicon nanocrystals and efficiently transferred to erbium ions. The penetration depth in the visible wavelength range has been determined both theoretically and experimentally and is of the order of a few microns, so that the pumping scheme must be chosen perpendicularly to the top surface (x direction as shown in figure 1). Furthermore, pumping from the top is more suitable for simulation since it can be designed to have a slight dependence in the propagation direction (z).

The modelling of the amplification scheme must account for the interaction between electronic levels and light propagation. Regarding the interactions between levels, let N_1, N_2, N_3, N_4 and N_5 be the populations of the ground level and the first four excited levels of erbium. N_{Si} and N_{ex} are the populations of the silicon nanograins and excitons respectively. The populations are governed by the following set of rate equations based on the Einstein

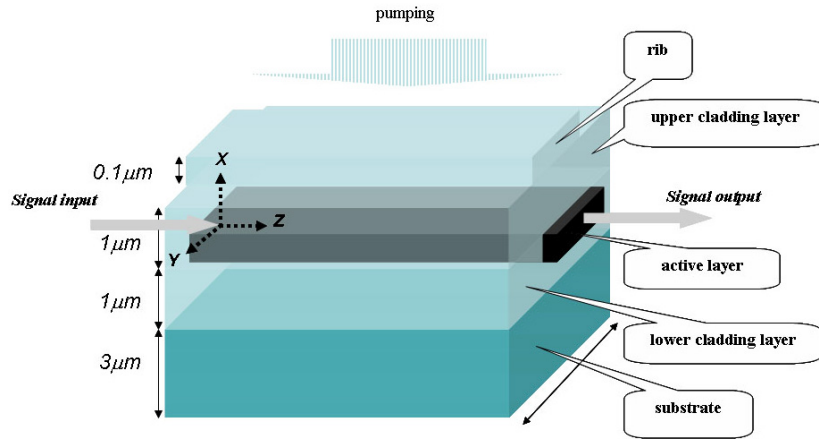


Figure 1. Scheme of the slab waveguide considered in the calculations. The optical indices have been taken equal to 3.0, 1.45, 1.8 and 1.45 for the substrate, the lower cladding layer, the active layer and the upper cladding layer respectively, according to experimental measurements.

(This figure is in colour only in the electronic version)

phenomenological approach for a system with known excitation levels. This approach has been used in the fundamental work of Strohhöffer and Polman [17] in Yb–Er codoped systems as well as in [15] for erbium and silicon codoped silica.

$$dN_{\text{ex}}/dt = \sigma_{\text{ng}}^{\text{a}} \Phi_{\text{p}} (N_{\text{Si}} - N_{\text{ex}}) - N_{\text{ex}}/\tau_{\text{ex}} - K_{\text{tr}} N_1 N_{\text{ex}} \quad (1)$$

where Φ_{p} is the flux of pumping photons (photon $\text{cm}^{-2} \text{s}^{-1}$), $\sigma_{\text{ng}}^{\text{a}}$ is the pumping photon absorption cross-section of silicon nanograins (cm^{-2}), τ_{ex} is the exciton lifetime (radiative + non-radiative) (s) and K_{tr} is the energy transfer coefficient to erbium ($\text{cm}^3 \text{s}^{-1}$).

It is supposed that only one exciton may be created by one incident photon within a silicon nanograin. In other words, the maximum number of excitons that can be created is equal to the number of silicon nanograins.

The rate equations governing the populations N_1 , N_2 , N_3 , N_4 and N_5 have been fully described in [15]. According to the approximations proposed (i.e. ultrafast decay from level 5 to 4 and from level 4 to 3), we can restrict our description to the populations N_1 , N_2 and N_3 :

$$dN_3/dt = K_{\text{tr}} N_1 N_{\text{ex}} + W_{\text{p}} N_1 - (A_{32} + A_{31}) N_3 + C_{\text{Er}}^{\text{up}} N_2^2 \quad (2)$$

$$dN_2/dt = W_{12} N_1 - (W_{21} + A_{21}) N_2 + A_{32} N_3 - 2C_{\text{Er}}^{\text{up}} N_2^2 \quad (3)$$

$$dN_1/dt = -K_{\text{tr}} N_1 N_{\text{ex}} - (W_{\text{p}} + W_{12}) N_1 + (W_{21} + A_{21}) N_2 + C_{\text{Er}}^{\text{up}} N_2^2 \quad (4)$$

where the transition probabilities W depend on the photon flux (Φ_{p} (*pump*) or Φ_{s} (*signal*)) via the following relationships:

$$W_{\text{p}} = \sigma^{\text{Er}} \Phi_{\text{p}} : \quad \text{absorption rate of Er at pump wavelength } (\lambda_{\text{p}} = 488 \text{ nm})$$

$$W_{12} = \sigma_{12} \Phi_{\text{s}} : \quad \text{absorption of Er at signal frequency } \nu_{\text{s}}$$

$$W_{21} = \sigma_{21} \Phi_{\text{s}} : \quad \text{stimulated emission of Er at signal frequency } \nu_{\text{s}}.$$

For the excitation of the coupled system,

$$A_{32} + A_{31} = 1/\tau_3^{\text{Er}} : \quad \text{lifetime of Er in the second excited state}$$

$$A_{21} = 1/\tau_2^{\text{Er}} : \quad \text{lifetime of Er in the first excited state}$$

$$C_{\text{Er}}^{\text{up}} : \quad \text{up-conversion coefficient } (\text{cm}^{-3} \text{s}^{-1}).$$

For given Φ_p and Φ_s fluxes, the population equations (1)–(3) are solved in the steady state ($dN_i/dt = 0$). The steady state value of N_3 (corresponding to $dN_3/dt = 0$) is injected into the other equations before being neglected regarding the other populations. We now deal with three equations (including equation (1)) to determine the populations N_1 , N_2 and N_{ex} , taking into account that

(i) the total erbium concentration N_{er} is given by

$$N_{er} = N_1 + N_2 \quad (5)$$

(ii) equation (2) now reduces to

$$dN_2/dt = K_{tr}N_1N_{ex} + W_{12}N_1 + W_pN_1 - (A_{21} + W_{21})N_2 - C_{Er}^{up}N_2^2. \quad (6)$$

Under these conditions, the steady state solution of (6) is therefore obtained by the solution of an equation of the third degree in N_2 .

Regarding light propagation, it must be noticed that the photon fluxes Φ_p and Φ_s depend in principle on the (x, y, z) coordinates and have to be analysed separately. The propagation of the pumping light along the x axis leads to multiple internal reflections on the interfaces between layers. Each layer is characterized by its thickness and complex dielectric function, while the dielectric function of the composite active layer is simulated by means of the Bruggeman effective medium approximation (BEMA) [18] as a function of composition. Propagation across the multilayered structure is calculated with a matrix procedure [19], allowing the profile along the x axis $\Phi_p(x)$ in the active guide to be determined. An incoherent source has been considered in the profile calculations. Pumping light does not propagate along the z axis and no boundary conditions are considered in the y direction.

Let us now consider the signal propagation. The signal Φ_s (photons $\text{cm}^{-2} \text{s}^{-1}$) propagates along the z axis according to the following equation (7):

$$d\Phi_s(x, y, z)/dz = (\sigma_{21}N_2(x, y, z) - \sigma_{12}N_1(x, y, z) - \alpha)\Phi_s(x, y, z) \quad (7)$$

α (cm^{-1}) accounts for all the optical losses except those due to erbium absorption.

The variables are separated so that $\Phi_s(x, y, z) = \phi_s(z)g(x, y)$. Here, $g(x, y)$ is the profile function (in cm^{-2}) of the signal. The signal intensity profile within the waveguide cross-section has been numerically investigated using the effective medium method and the scalar field approximation for both electric and magnetic field. This work is still being processed and will be published elsewhere. Therefore, concerning the calculations presented below, the $g(x, y)$ function has been fitted to the theoretical results using the product of two Gaussian functions that are maximal at the centre ($x = 0, y = 0$) of the waveguide cross-section S_{wg} . Moreover $g(x, y)$ is normalized over the guide section S_{wg} . Within this framework, the signal propagation equation can be expressed in terms of the power propagation $P_s(z)$ (in watts) along the z axis. $P_s(z)$ is linked to $\Phi_s(z)$ by

$$P_s(z) = h\nu_s \int \int_{S_{wg}} \Phi_s(x, y, z) dx dy = h\nu_s \phi_s(z) \int \int_{S_{wg}} g(x, y) dx dy = h\nu_s \phi_s(z).$$

The propagation equation (7) can be rewritten:

$$dP_s(z)/dz = P_s(z) \int \int_{S_{wg}} (\sigma_{21}N_2(x, y, z) - \sigma_{12}N_1(x, y, z) - \alpha)g(x, y) dx dy. \quad (8)$$

Since the signal power and the erbium level populations depend on one another, the solution of equations (1)–(8) is reached using an iterative process.

The first step consists in attributing initial values to the different populations as well as the powers in each slice Δz of the guide: $N_1(x, y, z) = N_{er}(x, y, z)$, $N_2(x, y, z) = 0$, $\Phi_s(z = 0) = \Phi_s(\text{input})$, $\Phi_s(z \neq 0) = 0$. $\Phi_p(x)$ has been described above and does not depend on z .

The propagation equations are solved along the guide, leading to new values of $\Phi_s(z)$ and to the value of $\Phi_s(z = L)$ at the output end of the guide. Then the population equations are solved in the steady state, giving new values of $N_1(x, y, z)$, $N_2(x, y, z)$ and $N_{\text{ex}}(x, y, z)$ from which we deduce the next value of $\Phi_s(z = L)$ using the propagation equations. This process stops when the relative difference in $\Phi_s(z = L)$ between two iterations is lower than 0.05%.

Following the procedure detailed above, the amplified spontaneous emission power is computed taking into account the emission and absorption spectra of erbium, leading to three contributions to the total noise figure described in [20]:

- the shot noise $V_{\text{shot}} = 2h\nu P_s(L) + 4N_2\Delta z \int \int h^2v^2\sigma_{21}(v) dv$;
- the signal-spontaneous noise $= P_s(L)4N_2\Delta zh\nu\sigma_{21}(v)$;
- the spontaneous-spontaneous noise $= 4(4N_2\Delta z)^2 \int \int h^2v^2\sigma_{21}^2(v) dv$.

The expressions above are integrated over the emission spectrum range. The total noise figure is the sum of these three components.

In the following section, gain and noise figure simulations are detailed through the investigation of the influence of different parameters: erbium and silicon nanograin concentrations, device length, pumping power signal power and signal confinement.

2. Simulations

The main physical parameters used in this section are the same as those used in [15]. Unless different values are specified in the following lines, the calculations presented hereafter have been performed with the parameters reported in table 1. The silicon excess Si_{exc} is defined as the ratio of the number of silicon atoms in excess to the total number of atoms (Si, Er and O) per unit volume. The value of Si_{exc} associated with a mean grain diameter D_g gives the concentration of silicon nanograins N_{Si} . Hereafter, D_g is taken as equal to 1.2 nm. Using the mean densities of $5 \times 10^{22} \text{ Si cm}^{-3}$ and $2.3 \times 10^{22} \text{ SiO}_2 \text{ cm}^{-3}$ and neglecting the volume occupied by the erbium ions, the silicon excess Si_{exc} and the silicon nanograin concentration $N_{\text{Si}} (\text{cm}^{-3})$ are linked by

$$N_{\text{Si}} = 1.53 \times 10^{21} \text{Si}_{\text{exc}} / (1 + 0.38\text{Si}_{\text{exc}}). \quad (9)$$

In the following figures, the Si_{exc} range between 5% and 45% corresponds to an N_{Si} range between $7.5 \times 10^{19} \text{ cm}^{-3}$ and $6 \times 10^{20} \text{ cm}^{-3}$.

The gain is computed for a device length of 1 cm except in section 2.2 where the influence of the length is investigated.

We consider that the up-conversion coefficient value used in the calculation ($7 \times 10^{-17} \text{ cm}^3 \text{ s}^{-1}$) is high. We can estimate the different terms of equation (6) and compare the mean value of $C_{\text{up}}N_2$ to $1/\tau_2^{\text{Er}}$ considering a mean N_2 value of the order of 10^{20} cm^{-3} :

$$C_{\text{up}}N_2 = 7 \times 10^{-17} \times 10^{20} = 14000 \text{ s}^{-1} \text{ whereas } 1/\tau_2 = 1/(4 \times 10^{-3}) = 250 \text{ s}^{-1}.$$

Hence the up-conversion mechanism is the main source of N_2 de-excitation. Furthermore, the transfer coefficient can also be considered as being high since, from equation (1), a comparison can be made between $K_{\text{tr}}N_1 (=2 \times 10^{-15} \times 10^{20} = 20000 \text{ s}^{-1})$ and $1/\tau_{\text{ex}} (=1/(50 \times 10^{-6}) = 20000 \text{ s}^{-1})$. In such a case the natural exciton decay time τ_{ex} is of the same order of magnitude as the decay time due to the energy transfer to erbium.

2.1. Erbium and silicon nanograin concentrations

2.1.1. Gain figure. The gain figure is reported as a function of silicon excess content and erbium ion concentration for given pumping powers (10 W cm^{-2} (figure 2(a)) and 30 W cm^{-2}

Table 1. Physical data used to simulate optical gain in a slab waveguide constituted of erbium ions and silicon nanograins embedded in a silica matrix.

Device length range	0.5–5.0 cm
Energy transfer coefficient	$2.0 \times 10^{-15} \text{ cm}^3 \text{ s}^{-1}$
Er pump absorption cross-section (cm^2) in the region of $\lambda_{\text{pump}} = 488 \text{ nm}$	$2 \times 10^{-24} \text{ cm}^2$
Erbium absorption cross-section spectrum in the signal wavelength range. Peak value at $\lambda = 1.533 \mu\text{m}$	$4.5 \times 10^{-21} \text{ cm}^{-2}$
Erbium concentration	10^{20} – 10^{21} cm^{-3}
Erbium emission spectrum. Peak value at $\lambda = 1.533 \mu\text{m}$	$4.9 \times 10^{-21} \text{ cm}^{-2}$
Intrinsic exciton metastable state lifetime	50 μs
Lifetime of doubly excited clustered pair	50 ns
Lifetime of the Er metastable level (referred to as N_2 in the text)	4 ms
Number of excitons simultaneously created within one silicon nanograin	1
Pump background losses	0.0 dB cm^{-1}
Pump input loss	0.0 dB
Pump power range	5–50 W cm^{-2}
Pump wavelength	488 nm
Signal and ASE background losses	2 dB cm^{-1}
Signal input loss	0.0 dB
Signal loss after amplifier section	0.0 dB
Signal power	2 mW
Signal wavelength	1.54 μm
Silicon excess	5%–45%
Silicon grain absorption cross-section (cm^2) in the region of $\lambda_{\text{pump}} = 488 \text{ nm}$. Peak value:	$2 \times 10^{-16} \text{ cm}^2$
Silicon grain diameter	1.2 nm
Up-conversion coefficient	$7.0 \times 10^{-17} \text{ cm}^3 \text{ s}^{-1}$

(figure 2(b)). On one hand, it is shown that for a given silicon excess content Si_{ex} the gain reaches a maximum value corresponding to an optimal erbium concentration (N_{er}) depending on Si_{ex} . On the other hand, for a given erbium concentration, increasing the silicon excess content is a good way to increase the gain. It is seen (figure 2(a), $P_{\text{pumping}} = 10 \text{ W cm}^{-2}$) that the best set ($N_{\text{er}}, \text{Si}_{\text{ex}}$) corresponding to a positive gain lies within the region where $15\% < \text{Si}_{\text{ex}} < 45\%$ and $1.5 \times 10^{20} \text{ cm}^{-3} < N_{\text{er}} < 5.5 \times 10^{20} \text{ cm}^{-3}$. This region strongly depends on the pumping power since for a positive gain and $P_{\text{pumping}} = 30 \text{ W cm}^{-2}$ (figure 2(b)) the N_{er} and Si_{ex} ranges become

$$6\% < \text{Si}_{\text{ex}} < 45\% \quad \text{and} \quad 1.1 \times 10^{20} \text{ cm}^{-3} < N_{\text{er}} < 1 \times 10^{21} \text{ cm}^{-3}.$$

2.1.2. Erbium inversion coefficient N_2/N_{er} . In parallel with the preceding figures, the erbium inversion coefficient is plotted versus N_{er} and Si_{exc} for two pumping powers, 10 W cm^{-2} (figure 3(a)) and 30 W cm^{-2} (figure 3(b)).

At low erbium concentrations ($\sim 10^{20} \text{ cm}^{-3}$) almost all the erbium ions are excited since $0.8 < N_2/N_{\text{er}} < 1$ even though the concentration N_2 itself is not high enough to achieve positive gain (figure 2). Moreover, for such concentrations, the gain decreases whereas the inversion coefficient increases. There is no contradiction because the absolute concentration N_2 is lower for $N_{\text{er}} = 1 \times 10^{20} \text{ cm}^{-3}$ than for $N_{\text{er}} = 4 \times 10^{20} \text{ cm}^{-3}$. Finally, it appears that the relevant data required to optimize the gain are the absolute concentrations of excited erbium (N_2) and the ratio N_2/N_{er} .

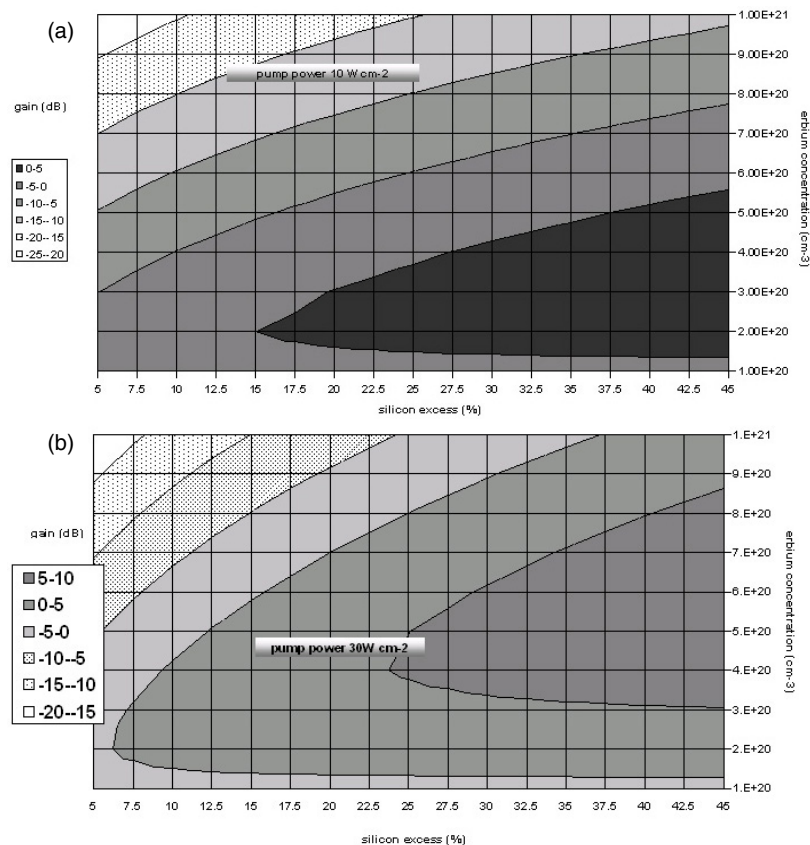


Figure 2. Signal gain in dB as a function of the silicon excess (in %) and the erbium concentration (in Er cm^{-3}). The corresponding lateral pumping powers are 10 W cm^{-2} (a) and 30 W cm^{-2} (b). The signal profile width is 510 nm.

At constant silicon excess, the increase of the erbium concentration (N_{er}) leads to a decrease of the inversion coefficient. For example, under a pump flux of 10 W cm^{-2} , for $\text{Si}_{\text{excess}} = 40\%$, the erbium concentration of $4 \times 10^{20} \text{ cm}^{-3}$ leading to a high gain (figure 2(a)) corresponds to a mean inversion coefficient between 0.6 and 0.8.

2.1.3. Number of inverted erbiums per silicon nanograin (N_2/N_{Si}). The number of inverted erbiums is plotted as a function of N_{er} and Si_{exc} for two pumping powers (10 W cm^{-2} (figure 4(a)) and 30 W cm^{-2} (figure 4(b))). Comparing these figures to the corresponding gain figures (figures 2(a) and (b)), the highest gains are obtained not for the highest values of N_2/N_{Si} but for an optimal value which lies below 0.5 excited erbium per silicon nanograin for $P_{\text{pump}} = 10 \text{ W cm}^{-2}$ and between 0.5 and 1 for $P_{\text{pump}} = 30 \text{ W cm}^{-2}$. It must be noticed that high values of N_2/N_{Si} refer to the lowest gain values because the concentration N_{Si} is not high enough. The reader should keep in mind that this ratio N_2/N_{Si} results from both propagation equations and steady state solutions of the population equations.

2.2. Pump power and device length

The gain figure is reported versus the pump power and device length in figure 5 for a silicon excess of 20% and an erbium concentration of $2 \times 10^{20} \text{ cm}^{-3}$. Two main comments can be

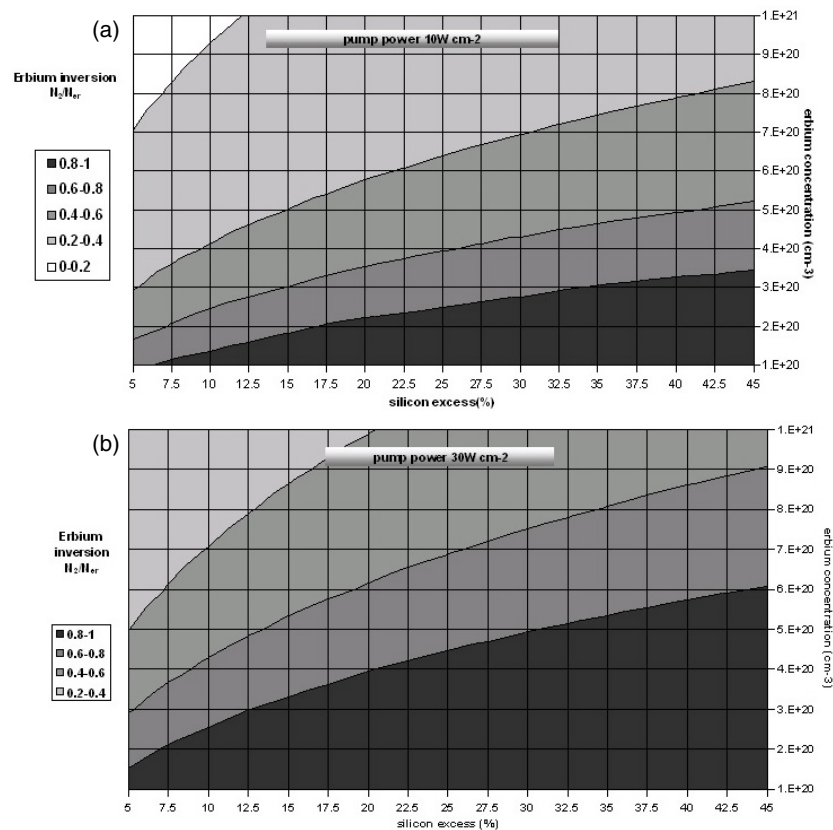


Figure 3. Erbium inversion coefficient (N_2/N_{er}) as a function of the silicon excess (in %) and the erbium concentration (in Er cm^{-3}). The corresponding lateral pumping powers are 10 W cm^{-2} (a) and 30 W cm^{-2} (b).

made. On one hand, for a given device length (higher than 0.8 cm), it is obvious that a gain increase requires a pumping power (Φ_p) increase. However, the gain reaches a saturation value for high Φ values. On the other hand, this figure points out the fact that there is a critical length ($l_{\text{crit}} = 0.8 \text{ cm}$) under which it is impossible to achieve positive gain upon increasing the pumping power. In this case, the total number of erbium ions (not only the concentration) is not high enough to allow the amplification of a given signal. Moreover, for a length lower than l_{crit} , the gain is a decreasing function of the pumping power.

2.3. Signal confinement

All the above results have been obtained with a signal power of 2 mW considering a Gaussian profile width (FWHM) of 500 nm . This parameter strongly affects the gain possibilities since a high power density can be reached with a low pumping power if the slab waveguide characteristics (geometry and layer optical indices) enable a high optical mode confinement. For a pumping power equal to 30 W cm^{-2} , a comparison can be made between the gain figure obtained with $\text{FWHM} = 500 \text{ nm}$ (figure 2(b)) and with $\text{FWHM} = 1000 \text{ nm}$ (figure 6). The 'area' corresponding to a positive gain is larger for narrow signal profile. Furthermore, a gain of 5 dB is reachable with $\text{FWHM} = 500 \text{ nm}$, in contrast to the case of a wider signal profile ($\text{FWHM} = 1000 \text{ nm}$).

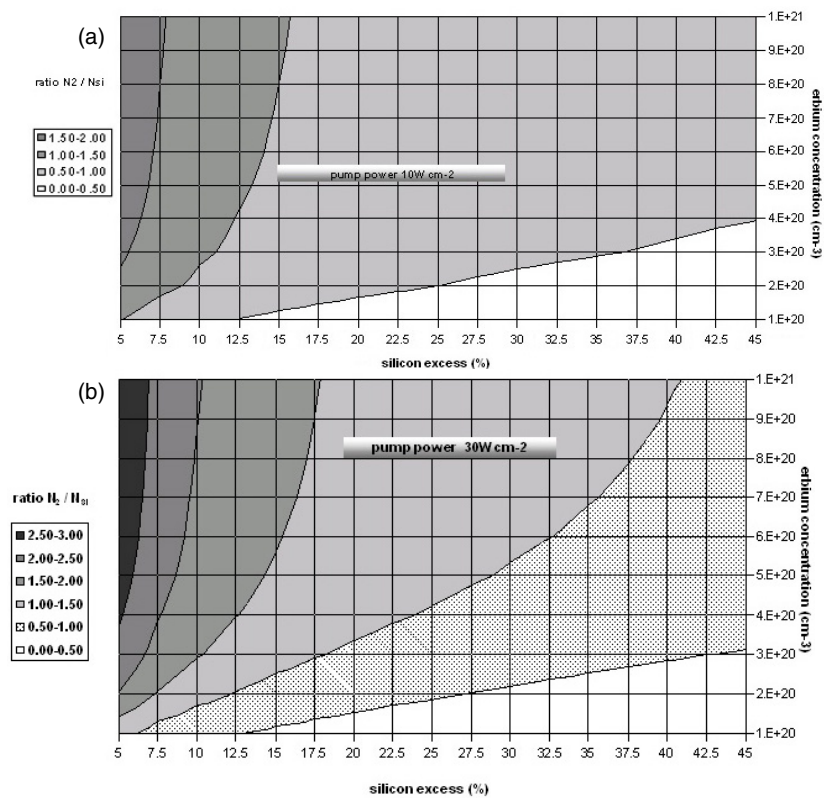


Figure 4. Ratio (N_2/N_{Si}) representing the number of excited erbium ions per silicon nanograin as a function of the silicon excess (in %) and the erbium concentration (in Er cm^{-3}). The corresponding lateral pumping powers are 10 W cm^{-2} (a) and 30 W cm^{-2} (b).

2.4. Noise figure

The noise figure is plotted versus the silicon excess and erbium concentration for two pumping powers: 10 W cm^{-2} (figure 7(a)) and 30 W cm^{-2} (figure 7(b)). This aspect is generally neglected in the simulations of optical device gain. Here, for a pumping power of 10 W cm^{-2} , it is shown that the region of positive gain values (between 0 and 5 dB) presented in figure 2(a) corresponds to the region of lowest noise (between 4 and 8 dB). This feature is thus not satisfactory since the noise is higher than the gain. This drawback disappears for higher pumping power (30 W cm^{-2} , figure 7(b)). In that case the comparison between figures 2(b) and 7(b) indicates that a high gain (5–10 dB) is reached in the range $3 \times 10^{20} \text{ cm}^{-3} < N_{er} < 9 \times 10^{20} \text{ cm}^{-3}$ and $25\% < Si_{ex} < 45\%$ —which is the range in which the noise (4–7 dB) is lower than the gain.

3. Conclusion

The issue of gain in optical devices based on silicon–silica films doped with erbium has been thoroughly investigated by solving within an iterative process the propagation equations of a $1.54 \mu\text{m}$ signal along a slab waveguide together with the population equations of the first three erbium levels coupled to those of the silicon nanograin and exciton populations. The influence

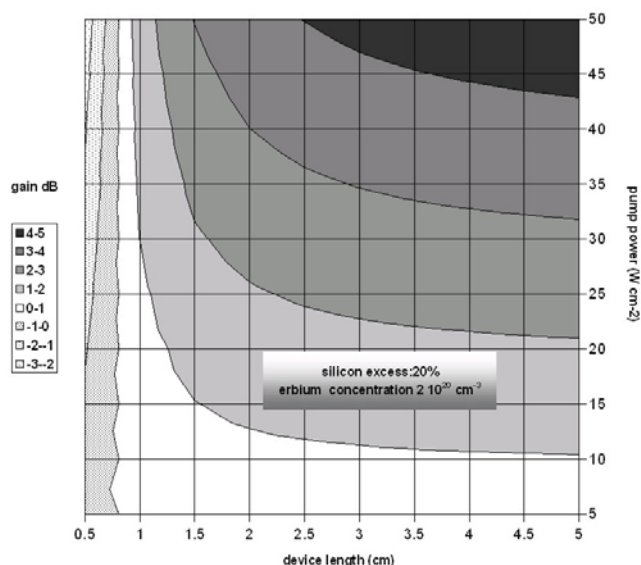


Figure 5. Gain (in dB) as a function of the device length and the pumping power for a given erbium concentration ($2 \times 10^{20} \text{ cm}^{-3}$) and 20% silicon excess.

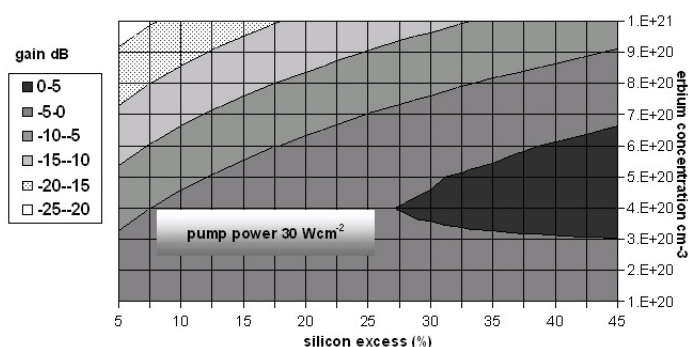


Figure 6. Signal gain in dB as a function of the silicon excess (in %) and the erbium concentration (in Er cm^{-3}) for a pumping power of 30 W cm^{-2} . The signal profile FWHM is 1000 nm as compared with FWHM = 500 nm in figure 2.

of the main parameters (erbium concentration, silicon excess, pumping power and device length) has been studied, leading to the definition of a best set required to obtain a positive gain higher than the noise. The quantitative gain and noise results given in this paper also depend on two parameters that have been kept constant and equal to the commonly admitted values in such systems: the up-conversion coefficient C_{up} ($=7 \times 10^{-17} \text{ cm}^3 \text{ s}^{-1}$) and the energy transfer efficiency K_{tr} ($=2 \times 10^{-15} \text{ cm}^3 \text{ s}^{-1}$) which have been considered as high values (see section 2).

Besides, the calculation code used in this article allows the possibility (which is not presented here) of simulating the effect of other parameters such as exciton lifetime τ_{ex} , the number k of excitons created by one incident pumping photon, the possible backtransfer of energy between the erbium N_4 level and a silicon nanograin, the signal losses at the input end of the device and the effect of erbium clustering that would lower the efficiency of energy transfer from silicon nanograin to the erbium ions.

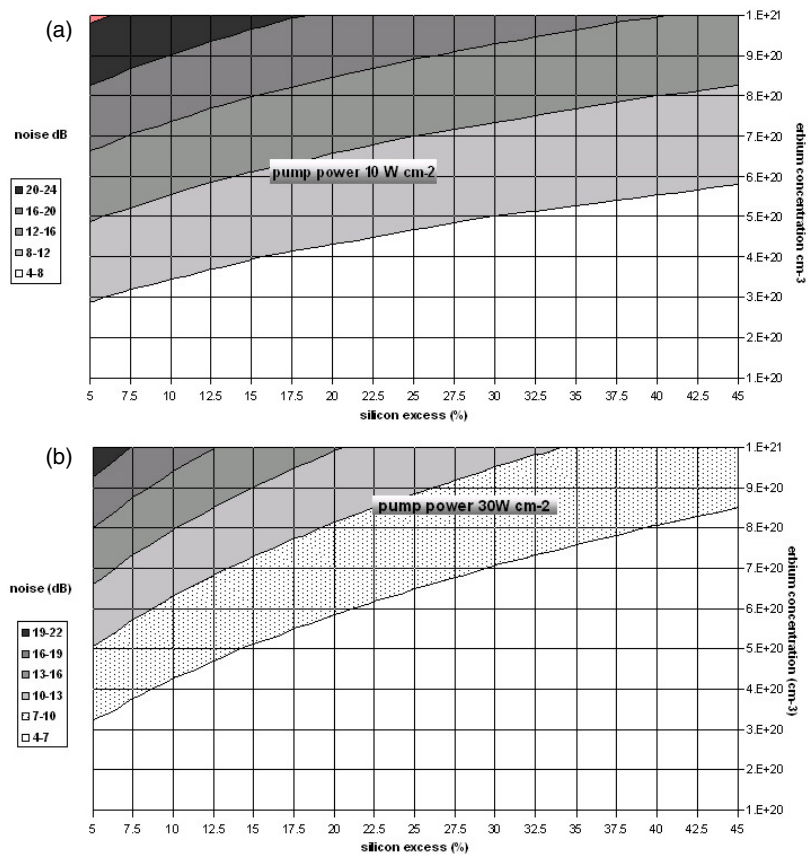


Figure 7. Noise figure (in dB) as a function of the silicon excess (in %) and the erbium concentration (in Er cm^{-3}). The corresponding lateral pumping powers are 10 W cm^{-2} (a) and 30 W cm^{-2} (b).

Acknowledgment

The authors acknowledge support from the SINERGIA European Union project IST-2000-29650. SINERGIA stands for Si nanocrystals and Er co-doped glasses for optical amplifiers.

References

- [1] Kik P G and Polman A 2003 *Towards the First Silicon Laser* ed L Pavesi (Dordrecht: Kluwer–Academic) pp 383–400
- [2] Iacona F, Franzò G and Spinella C 2000 *J. Appl. Phys.* **87** 1295
- [3] Shimizu-Iwayama T, Kurumado N, Hole D E and Townsend P D 1998 *J. Appl. Phys.* **83** 6018
- [4] Min K S, Shcheglov K V, Yang C M, Atwater H A, Brongersma M L and Polman A 1996 *Appl. Phys. Lett.* **69** 2033
- [5] Fauchet P M 1996 *J. Lumin.* **70** 294
- [6] Kenyon A J, Trwoga P F, Pitt C W and Rehm G 1996 *J. Appl. Phys.* **79** 9291
- [7] Khriachtchev L, Novikov S and Lahtinen J 2002 *J. Appl. Phys.* **92** 5856
- [8] Watanabe K, Fujii M and Hayashi S 2001 *J. Appl. Phys.* **90** 4761
- [9] Fujii M, Yoshida M, Kanzawa Y, Hayashi S and Yamamoto K 1997 *Appl. Phys. Lett.* **71** 1198
- [10] Kenyon A J, Chryssou C E, Pitt C W, Shimizu-Iwayama T, Hole D E, Sharma N and Humphreys C J 2002 *J. Appl. Phys.* **91** 367

-
- [11] Seo S-Y and Shin J H 2001 *Appl. Phys. Lett.* **78** 2709
 - [12] Kik P G and Polman A 2000 *J. Appl. Phys.* **88** 1992
 - [13] Kik P G, Brongersma M L and Polman A 2000 *Appl. Phys. Lett.* **76** 2325
 - [14] Kenyon A J 2002 *Prog. Quantum Electron.* **26** 225
 - [15] Pacifici D, Franzò G, Priolo F, Iacona F and Dal Negro L 2003 *Phys. Rev. B* **67** 245301
 - [16] Han H-S, Seo S-Y, Shin J H and Park N 2002 *Appl. Phys. Lett.* **81** 3720
 - [17] Strohhofer C and Polman A 2001 *J. Appl. Phys.* **90** 4314
 - [18] Bruggeman D A G 1935 *Ann. Phys., Lpz.* **24** 636
 - [19] Moreno J A, Garrido B, Samitier J and Morante J R 1997 *J. Appl. Phys.* **81** 1933
 - [20] Baney D M, Gallion P and Tucker R S 2000 *Opt. Fiber Technol.* **6** 122